

S1. TORSION UPDATE

Rotatable bonds are bonds that can split the molecule into two nonempty disjoint fragments. The whole molecular structure can be split into several disjoint fragments. The number of rotatable bonds depends on the specific structure of the considering ligand. However, we can set the upper bound of the number of rotatable bonds and select according to the rank of betweenness centrality.

We apply the M torsion updates in a given order of rotatable bonds. For each torsion update k , the torsion is applied on the fragment with less number of atoms. The torsion update k of atom i in the target fragment is as follows:

$$\mathbf{R}_k(\mathbf{r}_i) = \tilde{R}(\theta_k)(\mathbf{r}_i - \mathbf{r}_{k0}) + \mathbf{r}_{k0}, \quad (\text{S1})$$

where θ_k is the corresponding torsion angle of the k th rotatable bond, and \mathbf{r}_{k0} is the position of one fixed atom on the corresponding rotatable bond. The rotation operator \tilde{R} along a rotatable bond of angle θ reads

$$\tilde{R}(\theta) = I + \sin \theta K + (1 - \cos \theta) K^2, \quad (\text{S2})$$

where K depends on the unit vector along the rotation axis $\mathbf{k} = (k_x, k_y, k_z)$

$$K = \begin{pmatrix} 0 & -k_z & k_y \\ k_z & 0 & -k_x \\ -k_y & k_x & 0 \end{pmatrix}. \quad (\text{S3})$$

S2. INTERACTION ENERGY FUNCTION

In this section, we show the details in LJ potential and electrostatic potential which are determined here <https://github.com/ccsb-scripps/AutoDock-Vina>.

A. Details in LJ potential

Before calculation the LJ potential, the distance r_{ij} between atom i and j is smoothened according to whether these two atom spheres are overlapped or too far way as follows:

$$r_{ij} \rightarrow \begin{cases} r_{ij} - \alpha_s, & \text{if } r_{ij} > R_{ij} + \alpha_s, \\ r_{ij} + \alpha_s, & \text{if } r_{ij} < R_{ij} - \alpha_s, \\ r_{ij}, & \text{if } R_{ij} - \alpha_s < r_{ij} < R_{ij} + \alpha_s, \end{cases} \quad (\text{S4})$$

where R_{ij} is the sum of radius of atom i and j , and α_s is a smoothing constant usually set to 0.25.

The depth of the potential well of atom i and j is determined as follows:

$$\varepsilon_{ij} = \sqrt{\varepsilon_i \varepsilon_j}, \quad (\text{S5})$$

where $\varepsilon_i, \varepsilon_j$ is the depth of the potential well of each atom, whose value depends on the atom type.

The values of radius and depth of the potential well of the element types included in the testing dataset are shown in Table S1.

In addition, V_{LJ}^{ij} is upper bounded by $V_{\max} = 100000$ and $V_{LJ}^{ij} = 0$ if $r_{ij} > r_{\max} = 8\text{\AA}$. The weight of LJ potential is given as $w_1 = 0.1406$.

B. Details in electrostatic potential

The correction function $f(r_{ij})$ of r_{ij} is as follows:

$$f(r_{ij}) = \frac{1}{332} \left(-8.5525 + \frac{86.9525}{1 + 7.7839e^{-0.3153r_{ij}}} \right). \quad (\text{S6})$$

In addition, $1/r_{ij}$ is upper bounded by 100000 and $V_e^{ij} = 0$ if $r_{ij} > r_{\max} = 20.48\text{\AA}$. The weight of electrostatic potential is given as $w_2 = 0.1662$.

TABLE S1. Values of radius and depth of the potential well of the element types included in the testing dataset.

atom type	radius	depth of potential well ε
C	2.000	0.150
O	1.600	0.200
N	1.750	0.160
S	2.000	0.200
H	1.000	0.020
P	2.100	0.200
I	2.360	0.550
F	1.545	0.080
Br	2.165	0.389
Cl	2.045	0.276
Fe	0.650	0.010

S3. IMPLEMENTATION DETAILS OF DOCKING APPROACHES

A. Implementation details

In re-docking scenario, the conformation is fixed as the crystal structure. In self-docking scenario, the initial conformation is given by RDKit.

In QMD, the search space is a $6 \times 6 \times 6 \text{ \AA}^3$ box centered at the initial location of the ligand. The initial locations are randomly generated under the uniform distribution in the $6 \times 6 \times 6 \text{ \AA}^3$ box centered at the ground-truth. Hence the whole search space for QMD is a $12 \times 12 \times 12 \text{ \AA}^3$ box. The initial rotation angles of the ligand are randomly generated by the uniform distribution over the rotation range $[-\pi, \pi)$. The number of rotatable bonds is set at most three. The search range of the torsion angle is set $[-\pi/16, \pi/16)$ since the average RMSD between the crystal conformation and the conformation optimized by RDKit of the testing dataset is only 0.85 \AA . The degrees of freedom of translation and rotation are encoded by four binary variables each and the degree of freedom of torsion is encoded by two binary variables. Thus the step sizes of translation, rotation and torsion are $\Delta T = 0.375 \text{ \AA}$, $\Delta\phi = 22.5^\circ$, and $\Delta\theta = 5.625^\circ$. In perturbation detection, we set the small difference about $\delta = 0.5\%$. For those within δ difference of the lowest energy, the best pose is the one with the smallest standard deviation. In general, to realize larger search space in pocket docking, we can divide it into smaller boxes and run our approach in parallel for each box with several random initial poses.

In Autodock Vina, the search space is a $12 \times 12 \times 12 \text{ \AA}^3$ box centered at the ground-truth. The initial location is generated by a random translation from the location of the ground-truth, and the initial rotation angles of the ligand are randomly generated under the uniform distribution over the rotation range $[-\pi, \pi)$. The parameter "exhaustiveness" is set to be 10, which means randomly sample 10 initial pose for each task.

In DIFFDOCK, the initial location is generated by a random translation from the location of the ground-truth under a uniform distribution $[-6, 6] \text{ \AA}$.

B. Search space

Here we make some remarks of the search space in Autodock Vina. The choice of search space strongly effects the behaviour of Autodock Vina.

We find that Autodock Vina shows better success rate if the center of the search space is closer to the ground-truth, which means this method prefers to search the center of the search space. Suppose the search space is a $20 \times 20 \times 20 \text{ \AA}^3$ box. When we randomly move the search space center away from the ground-truth within 2, 5, 7.5 and 10 \AA in three dimensions, the top-1 success rates are 31.75%, 27.02%, 20.61% and 10.58%, respectively. This implies that even though the ground-truth is in the search space, Autodock Vina can not succeed if the ground-truth is in the corner or far away from the center.

Autodock Vina restricts the whole ligand structure to be inside the search space. The default search space in Autodock Vina, SMINA and GNINA is an automatic box around the ligand with the default buffer of 2 \AA on all 6 sides. Under this setting, the top-1 success rate is about 7% higher than the setting of $12 \times 12 \times 12 \text{ \AA}^3$ search box centered at the ground-truth. This setting has already utilized the information of the ground-truth pose and will prefer the pose near the ground-truth. Otherwise, if the ligand is in a totally different orientation and far away from

TABLE S2. Average runtime for Autodock Vina, DIFFDOCK and QMD.

Methods	Avg. time	Device
Autodock Vina	2033 (± 5503) s	1-CPU
DIFFDOCK (train)	18 days	4-GPU
DIFFDOCK (inference)	10 s	1-GPU
QMD	4468 (± 3451) s	1-CPU

the center, the whole ligand structure is partly outside the search box, which may be forbidden in Autodock Vina. Therefore, the ground-truth is more likely to be found because of the restriction of the search space.

However, in our QMD, we do not have such restriction. The search space is only a restricted space for the center of the ligand instead of the whole ligand structure. QMD allows more possibilities of poses to be explored.

In this work, to compare with Autodock Vina as fair as possible, we set the search space to be $12 \times 12 \times 12 \text{ \AA}^3$ box centered at the ground-truth. This is a more general and natural setting in the real docking experiments.

S4. MACHINES AND RUNTIME DETAILS OF DOCKING APPROACHES

The average runtime and devices used are shown in Table S2. In DIFFDOCK, the final score model was trained on four 48GB RTX A6000 GPUs for 850 epochs around 18 days, and the confidence model was trained on a single 48GB GPU [?]. We directly utilize the trained model. The inference time of DIFFDOCK is calculated by us on a NVIDIA A100-SXM-80GB GPU when generating 10 samples. Autodock Vina (realized by ODDT) and QMD are run on the platform for running based on NUMA nodes, featuring 32 Intel(R) Xeon(R) CPUs E7-8890 v4 @ 2.20GHz. The runtime of Autodock Vina and QMD is the time for per prediction which runs on one CPU when generating 10 samples. However, the Autodock Vina engine within ODDT is run by C++ compared with QMD by Python. QMD does not need any pre-training or pre-calculating. The runtime of QMD is the whole end-to-end calculation time, which can be furthered reduced if consider further optimization to run a GPU.

Additionally, in QMD all variables can be simultaneously updated at each iteration step if parallel computation is used. But for the current computational cost shown in Table S2, the difference defined in Eq. (15) in the main text is calculated one by one and then update all variables. Therefore the time cost of QMD can be theoretically reduced by the times of the number of variables if parallel computation is used to calculate the difference.

S5. SELF-DOCKING VISUALIZATION

In this section, we show two examples of the self-docking predictions from QMD. The complexes are 6oxy and 6g2b. We show the RMSDs and scores of the top 5 predictions in Table S3 and Table S4 for 6oxy and 6g2b, respectively. Recall that the score function is the same as interaction energy function. The higher ranked prediction has lower score.

For 6oxy, the score of the ground-truth is -4.21. The higher ranked prediction basically has smaller RMSD, which is effective to find the best prediction close to the ground-truth. However, the top-1 prediction still has lower score than the ground-truth.

TABLE S3. The RMSDs and scores of the top-5 predictions of 6oxy.

Rank	RMSD	Score
1	0.89	-4.44
2	0.91	-4.43
3	5.51	-3.80
4	9.57	-3.64
5	4.93	-3.34

For 6g2b, the score of the ground-truth is -5.52. The top 2 predictions have the lowest scores but the corresponding RMSDs are larger than the other predictions. Therefore, the top-1 prediction is also reasonable and worth testing in the forward experiments. The top 5 predictions include the near-ground-truth prediction.

TABLE S4. The RMSDs and scores of the top-5 predictions of 6g2b.

Rank	RMSD	Score
1	4.77	-6.16
2	4.37	-5.87
3	0.54	-5.76
4	0.60	-5.75
5	0.47	-5.69

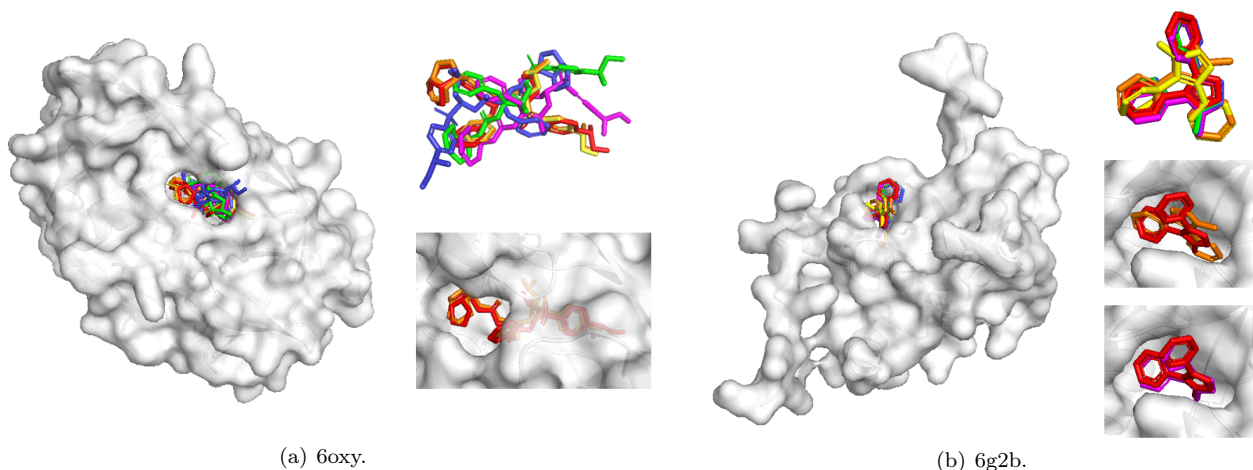


FIG. S1. Two examples of self-docking. The ground-truth pose is colored red, and the top 5 predictions are colored orange, yellow, green, blue and magenta, in the order of the rank. Shown are the predictions with and without the protein. The top-1 prediction (orange) and top-5 prediction are shown with the protein. (a) 6oxy. Top-1 and top-5 predictions are the same (orange). (b) 6g2b. Top-5 prediction is ranked no.5 (magenta).

QMD is capable to find a ranked pool of hypotheses of favorable-scoring predictions which are valid and reasonable as shown in Fig. S1. The ground-truth pose is colored red, and the top 5 predictions are colored orange, yellow, green, blue and magenta, in the order of the rank. We show the predictions with and without the protein. The top-1 prediction (orange) and top-5 prediction (i.e., the prediction with the smallest RMSD among the top 5) are shown with the protein. For 6oxy, top-1 and top-5 predictions are the same; for 6g2b, top-5 prediction is ranked no.5 (magenta).